Threshold Behavior in Formation of Optical Hexagons and First Order Optical Phase Transition

Serguey G. Odoulov, Mikhail Yu. Goulkov, and Oksana A. Shinkarenko
Institute of Physics, National Academy of Sciences, 03650, Kiev-39, Ukraine
(Received 7 April 1999)

The dynamics of optical hexagon excitation is studied experimentally in photorefractive barium titanate. The hard mode of the oscillation onset is discovered as well as a pronounced hysteresis loop in the dependence of the hexagon intensity on the crystal coupling strength. The analogy of excitation threshold of optical hexagon and first order optical phase transition is confirmed.

PACS numbers: 42.65.Hw, 42.65.Pc, 42.65.Sf, 47.54.+r

Starting from publication of Haken [1] it has become clear that the onset of oscillation in lasers can be considered as a kind of nonequilibrium optical phase transition. Below the threshold an active medium emits spontaneous radiation with a rather broad spectrum; the angular distribution of the emitted light is uniform in a 4π steradian solid angle. Above the threshold considerable narrowing is observed for both the temporal and the spatial spectra of radiation.

The control parameter of phase transition in lasers is the pump intensity; the normalized laser intensity may be considered an order parameter. For a free-running solid state laser the oscillation intensity is zero exactly at the threshold, i.e., the order parameter changes continuously from zero to finite value in the vicinity of transition. This behavior is typical for the second order phase transition.

A critical slowing down of fluctuations has been observed near the threshold, and critical indices (close to unity) were evaluated, also pointing to the second order phase transition [2]. At the same time a laser with the bleachable dye in the cavity (Q switched) exhibits the hard onset of oscillation, with a discontinuous jump of intensity to a certain finite level at threshold; this behavior is analogous to the first order transition.

Recently the analogy with phase transition was discussed also for coherent oscillators based on nonlinear wave mixing in photorefractive crystals [3,4]. In photorefractive coherent oscillators the temporal frequency of radiation is nearly the same as the frequency of the pump wave. The changes in the spatial distribution of radiation, however, are as large as in usual lasers: A highly collimated light beam is generated above the threshold, while wide-angle light-induced scattering is observed below the threshold. Above the threshold a single high-amplitude 3D refractive index grating replaces a multitude of small-amplitude, arbitrarily oriented "noisy" gratings existing below threshold.

For photorefractive oscillators the control parameter is the coupling strength (coupling coefficient γ times interaction length ℓ). With the order parameter, one can choose either the diffraction efficiency of the developing grating or the phase conjugate reflectivity (both quantities are zero below the threshold and saturate to unity for lossless optimized cavity, with increasing $\gamma\ell$).

A number of possible optical configurations of the photorefractive coherent oscillators [5,6] are much larger than that of usual lasers: Their optical cavities can be open; the oscillation may occur without any cavity. This results in a larger variety of physical properties of oscillators which we discuss further.

Until now the threshold behavior of two coherent photorefractive oscillators was considered from the point of view of the similarity to phase transition: of the ring-loop oscillator and the double phase conjugate mirror (DPCM). It has been shown that the onset of oscillation in these configurations of coherent oscillators has features similar to the second order phase transitions [3,4].

The purpose of this paper is to show that some photorefractive oscillators exhibit the threshold behavior similar to the *first order phase transitions* in a natural way, even without any Q switch inside the optical cavity. This statement is proved with a particular example of hard excitation of optical hexagons in a photorefractive crystal [7]—a kind of mirrorless coherent oscillation with frequency-degenerate backward wave four-wave mixing.

Three typical calculated dependences of the oscillation intensity on coupling strength were reported for photorefractive oscillators [5,6,8]. The first one shown in Fig. 1a is characteristic for the oscillators with closed cavities (such as Fabry-Perot or ring cavity), for the ring-loop oscillator and for the DPCM [5,6]. In these oscillators the output intensity (and phase conjugate reflectivity) is zero exactly at the threshold coupling strength $\gamma\ell_{\text{th}}$ and it gradually increases with increasing $\gamma\ell$. In such a way there is no discontinuity in the order parameter in the vicinity of the threshold.

The second known solution for the output intensity is shown in Fig. 1b; it is characteristic for the semilinear oscillator and for the Feinberg' Cat Conjugator [5,6]. The dependence on coupling strength is double valued here and it does not intersect the abscissa at any finite $\gamma\ell$ value. These oscillators need a certain seeding radiation to be switched on; usually the light-induced scattering is sufficient to start the oscillation [9].

0031-9007/99/83(18)/3637(4)$15.00

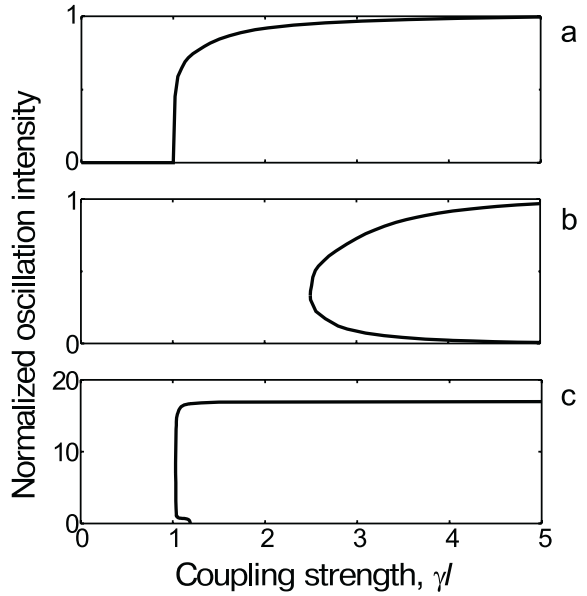

FIG. 1. Calculated coupling strength dependence of oscillation intensity normalized to pump intensity for the (a) ring-loop oscillator, (b) semilinear oscillator, and (c) ring-loop oscillator with photorefractive amplifier inside the cavity.

The third type of solution (Fig. 1c) was first obtained for the ring-loop oscillator with a photorefractive amplifier inside the loop [8]. Here the exact value of threshold $\gamma\ell_{\text{th}}$ exists but the solution is double valued for a certain interval of $\gamma\ell$ below the threshold. The results of recent calculation [10] indicate the same type of solution also for the excitation of optical hexagons in photorefractive crystals. Similar solutions are also known for optical hexagons in Kerr or resonant media [11–13].

One of the arguments used to prove the analogy between the oscillation onset in DPCM and second order phase transition [4] is the similarity of equations describing the two processes. The steady-state solution for the DPCM phase conjugate reflectivity, $|A_{\text{pc}}/A_s| = a$, is [6]

$$a = \tanh[a\gamma\ell/\gamma\ell_{\text{th}}], \tag{1}$$

where A_{pc} and A_s are the complex amplitudes of the phase conjugate (oscillation) wave and signal wave, respectively. By substituting $a \to M/M_\infty$, $\gamma\ell \to T^{-1}$, and $\gamma\ell_{\text{th}} \to T_c^{-1}$, one can obtain the equation describing the ferromagnetic phase transition [14],

$$M/M_\infty = \tanh[MT_c/M_\infty T], \tag{2}$$

where M is the magnetization, M_∞ is the ultimate magnetization when all spins are aligned, T is the temperature, and T_C is the Curie temperature.

Both Eqs. (1) and (2) describe the second order phase transition with the continuous variation of the order parameter ($|A_{\text{pc}}/A_s|$ and/or M/M_∞) near the critical point (see Fig. 1a). It should be emphasized, however, that for some other photorefractive oscillators (e.g., for the semilinear oscillator) Eq. (1) is still valid for a certain variable a, but this a is related to $|A_{\text{pc}}/A_s|$ in a much more complicated manner [5]. This results in quite a different solution for oscillation intensity (Fig. 1b), resembling the first order phase transition.

It is obvious that for the second and third types of solution (Figs. 1b and 1c) a hard excitation of the oscillation occurs, i.e., the oscillation starts at the threshold from a certain finite intensity. This behavior is similar to the first order phase transition; at the threshold $\gamma\ell_{\text{th}}$, both the derivative of the order parameter and the order parameter itself undergo the discontinuous change.

The characteristic feature of first order phase transition is the hysteresis effect. This can be easily seen, e.g., from the calculated dependence of Fig. 1c: When increasing the coupling strength one can switch on the oscillation only at $\gamma\ell_{\text{th}}$, but for the decreasing coupling strength the oscillation persists at $\gamma\ell < \gamma\ell_{\text{th}}$.

Below we describe the first observation of new features of optical hexagons in photorefractive $BaTiO_3$:Co including the well-developed hysteresis loops near the threshold of excitation.

The hexagons appear when the focused light beam of an Ar^+ laser illuminates the 2-mm-thick Z-cut sample and the highly reflecting flat mirror is placed just behind the sample to produce the counterpropagating pump wave [7]; see Fig. 2a. The distance L between the sample and mirror M is about 1 mm, so that not only the pump wave but also the generated sidebands of the hexagon are reflected back into the interaction region of nearly 300 μm diam. (The angular separation of the sidebands from the pump beam is about 1°.) The sample is tilted roughly to 45° to pump waves to profit from the large electro-optic constant r_{42} of $BaTiO_3$ and to diminish the losses for Fresnel reflection.

The excitation of hexagons as shown in Fig. 2b is observed at all blue and green Ar^+-laser wavelengths tested. The interaction is strongly nonlinear: multiple high orders (up to $3\mathbf{K}_\perp$ and $\sqrt{12}\,\mathbf{K}_\perp$, where $\mathbf{K}_\perp$ is the transverse

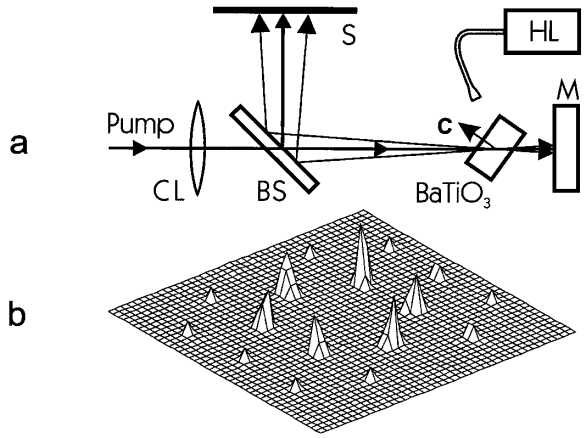

FIG. 2. Experimental setup (a) and 3D plot of the steady-state far-field intensity distribution on a screen S (b). CL is a converging lens, BS is a beam splitter, M is a mirror, and HL is a halogen lamp.

grating vector of the principal hexagon) are observed on the screen in steady state apart from six main spots.

If the photoconductivity of photorefractive crystal is higher than dark conductivity (which is usually the case) the coupling strength $\gamma\ell$ is independent of the light intensity. We introduce the intensity dependence of $\gamma\ell$ artificially by illuminating the sample with the auxiliary incoherent light from a halogen lamp (HL in Fig. 2). The intensity of an additional illumination is chosen in such a way as to ensure the comparable photoconductivities from the laser light and from incoherent light. The intensity dependence of $\gamma\ell$ is measured directly from the beam coupling of two counterpropagating pump waves, with the same experimental setup. No mechanical action is necessary to change $\gamma\ell$ in this technique; this results in better stability of optical setup and allows for easy detection of the threshold behavior.

Figure 3 shows the coupling strength dependence of one hexagon spot for the increasing (open squares) and decreasing (filled dots) coupling strength for different spacing L between the sample and feedback mirror.

One can see from Fig. 3 that (i) the oscillation starts discontinuously, i.e., the intensity of the hexagon spot is finite just above the threshold (hard mode of excitation); (ii) the threshold value of the hexagon intensity is roughly independent of L; (iii) the threshold coupling strength, however, is obviously increasing with the spacing; (iv) a distinct difference exists between the coupling strength where the oscillation starts for the increasing $\gamma\ell$ and where oscillation disappears for the decreasing $\gamma\ell$ (optical bistability, hysteresis); (v) the hysteresis loop becomes more narrow with increased spacing.

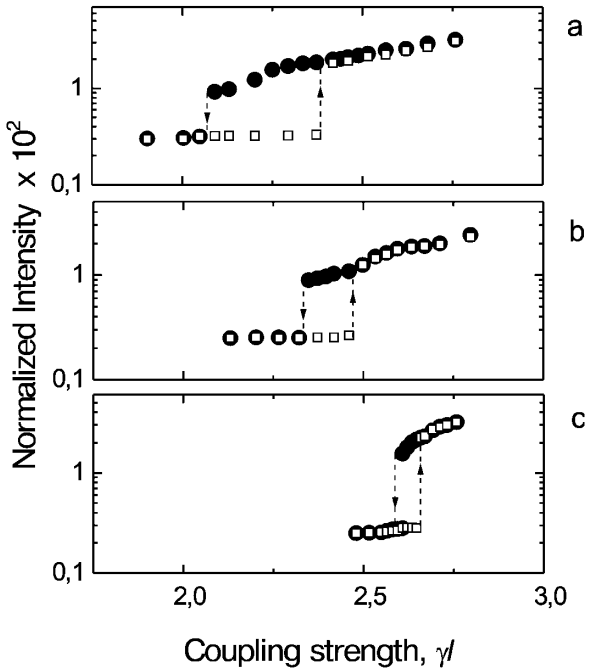

FIG. 3. Coupling strength dependence of hexagon intensity normalized to the input wave intensity. $L = 1.3$, 1.8, and 2 mm for a, b, and c, respectively.

The theory [10] predicts the hard mode of excitation with the explosion-type development of the hexagon structure. The calculated threshold $\gamma\ell_{\text{th}}$ is increasing with the increasing L (see branch 1 in Fig. 3 of [10]). In our experiment this increase of $\gamma\ell_{\text{th}}$ can have one more reason: the larger the L, the smaller the spatial overlap of the reflected side lobes with the pumped area becomes, i.e., the losses become larger.

The computer simulation for the initial intensity of the hexagon spot at the threshold, normalized to the forward pump intensity, gives 0.06–0.05 for the experimental interval of L variation. The measured values are 5–6 times smaller; the discrepancy can be explained in part by different losses not taken into account in the calculation (due to crystal absorption, Fresnel reflection from the sample faces, etc.). At the same time, the simulation predicts relatively weak dependence of the threshold hexagon intensity on L, in good qualitative agreement with the experiment.

The hard excitation of optical hexagons in photorefractive crystal should have a particular temporal development as follows from the calculations of Ref. [10]: After the beginning of exposure of a virgin sample (with all previously recorded photorefractive gratings erased) at first a pronounced conical light-induced scattering appears (ring on the screen). Within the linear stability analysis this corresponds to the growth of intensity of a large number of oblique beams. The intensity distribution in the ring is arbitrary and depends on fluctuations of the seeding radiation.

For well-developed scattering the interaction between particular components of scattered light becomes important. If, by chance, three components are present with the transverse wave vectors $\mathbf{K}_{\perp j}$, making the angles $\pi/3$ to each other, the evolution of the field amplitude A_j for every component is governed by the equation [10]

$$\partial A_j/\partial t = \nu A_j + UA_j^2, \tag{3}$$

where ν is an increment (growth rate of the linear instability) and U is the matrix element for the interaction of three hexagon side bands. For finite amplitude of the initial seed $A_j(t = 0) = A_{j0}$, the solution of Eq. (3) is

$$A_j = A_{j0}\nu/[(\nu + UA_{j0})\exp(-\nu t) - UA_{j0}], \tag{4}$$

i.e., for a certain $t_{\text{cr}} > 0$ the explosion-type growth of intensity to infinite value is predicted.

This solution is obtained in undepleted pump approximation; the ultimate intensity of all hexagon spots cannot become larger than the input pump intensity. In fact, the intensity of the hexagon spots saturates at much smaller values because of the development of high orders, which stabilize, according to [10], the hexagon intensity. In a formal way the additional terms, with higher powers of A_j, appear in Eq. (3) which results in the modification of the solution.

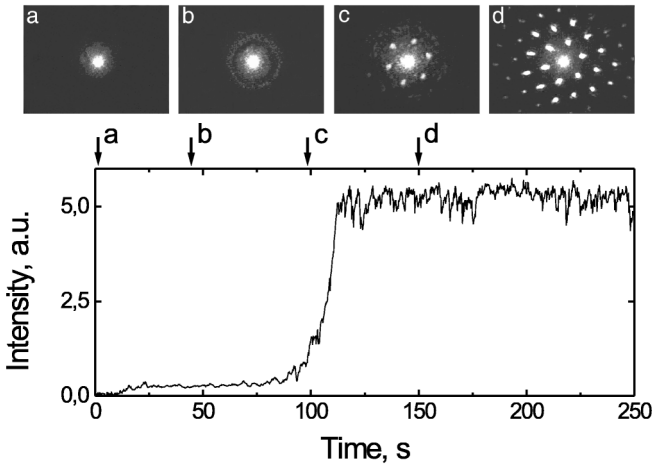

FIG. 4. Temporal dynamics of light intensity scattered along the conical surface where hexagon self-develops. Patterns a, b, c, and d correspond to particular exposure times shown by arrows.

Figure 4 represents the temporal development of the light intensity scattered along the cone with the apex angle equal to the largest angular separation of two hexagon spots. The pictures show the far-field intensity distribution for several characteristic exposure times.

It is quite obvious that details of the described calculation are confirmed by the experimental observations. Let us emphasize the two most important: (i) The characteristic time intervals, one with nearly uniform ring-shaped light-induced scattering and the other with pronounced hexagonal patterns are well separated from each other by the steplike change in intensity (hard excitation); (ii) the steady-state far-field intensity distribution contains more than 36 well-detectable spots (higher orders stabilize the hexagon intensity).

All experimental results presented in this Letter show that the optical hexagon emerges from the noise at threshold with certain finite intensity. Thus, the regular refractive index gratings which couple the hexagon side bands to the pump waves appear at threshold also with nonzero diffraction efficiency, i.e., discontinuously. Together with the detected optical bistability in the coupling strength dependence of hexagon intensity, this proves unambiguously the observation of *first order optical phase transition.*

The subcritical bifurcation seems to be a universal feature of hexagon formations wherever they are observed [15], in fluid mechanics as well as in optics. It should be emphasized, however, that the origin of optical hexagons in our experiment is quite different from that considered in [11–13]. Usually the diffraction inside the slice of nonlinear medium is neglected and diffusion is supposed to wash out the gratings formed by counterpropagating waves [16]. In the considered experiment just the reflection gratings couple the hexagon side lobes to counterpropagating pump waves because of the special choice of interaction geometry. Furthermore, the transverse intensity variation (in a plane normal to the pump waves) does not affect the refractive index in Z-cut $BaTiO_3$, as distinct from media with Kerr-type nonlinearity and saturation nonlinearity, where hysteresis was previously considered and observed. Thus the first experimental observation of the subcritical behavior of photorefractive hexagons reported in this Letter confirms that this type of bifurcation diagram is intrinsic to all hexagonal patterns. In the main context of our work it points to first order phase transition for this specific photorefractive oscillator.

Less pronounced hysteresis was detected for the Feinberg' Cat Conjugator [17] and for the semilinear coherent oscillator [18], indicating that these oscillators are also optical analogies of first order phase transition.

Financial support from the Civilian Research and Development Foundation (UP2-322) and from the Ministry for Science and Technology, Ukraine, is gratefully acknowledged. We thank D. Rytz for supplying us with an excellent sample of $BaTiO_3$, and M. Segev, B. Sturman, V. Obukhovsky and P. Lushnikov for helpful discussions.

[1] H. Haken, Rev. Mod. Phys. **47**, 67 (1975).
[2] M. Corti and V. Degiorgio, Phys. Rev. Lett. **36**, 1173 (1976).
[3] M. Goul'kov, S. Odoulov, and R. Troth, Ukr. Phys. J. **36**, 1007 (1991).
[4] D. Engin, S. Orlov, M. Segev, G. Valley, and A. Yariv, Phys. Rev. Lett. **74**, 1743 (1995).
[5] S.-K. Kwong, M. Cronin-Golomb, and A. Yariv, IEEE J. Quantum Electron. **22**, 1508 (1986).
[6] B. Fischer, S. Sternklar, and S. Weiss, IEEE J. Quantum Electron. **25**, 550 (1989).
[7] T. Honda, Opt. Lett. **18**, 598 (1993); T. Honda and H. Matsumoto, Opt. Lett. **20**, 1755 (1995); C. Denz, M. Schwab, M. Sedlatschek, T. Tschudi, and T. Honda, J. Opt. Soc. Am. B **15**, 2057 (1998), and references therein.
[8] V. Bazenov, S. Lyuksyutov, S. Odoulov, and M. Soskin, Sov. J. Quantum Electron. **19**, 910 (1989).
[9] A. Mamaev and A. Zozulya, Opt. Commun. **79**, 373 (1990).
[10] P. M. Lushnikov, J. Exp. Theor. Phys. **86**, 614 (1998).
[11] D. G. D'Alessandro and W. J. Firth, Phys. Rev. Lett. **66**, 2597 (1991); Phys. Rev. A **46**, 537 (1992).
[12] J. Y. Courtois and G. Grynberg, Opt. Commun. **87**, 186 (1992); A. Petrossian, M. Pinard, A. Maitre, J.-Y. Courtois, and G. Grynberg, Europhys. Lett. **18**, 689 (1992).
[13] T. Ackemann, B. Giese, B. Schaepers, and W. Lange, J. Opt. B **1**, 70 (1999).
[14] L. Landau and E. Lifshitz, *Statistical Physics* (Pergamon Press, Oxford, 1958).
[15] M. C. Cross and P. C. Hohenberg, Rev. Mod. Phys. **65**, 851 (1993).
[16] The only exception we know is the hexagon formation in gases (see, e.g., [12], where both the transmission and reflection gratings may appear simultaneously).
[17] J. Rodriguez, A. Siahmakoun, and G. Salamo, Appl. Opt. **26**, 2663 (1987).
[18] Sze-Keung Kwong, Mark Cronin-Golomb, and A. Yariv, Appl. Phys. Lett. **45**, 1016 (1984).